

Electric Vehicle Speed Control using Three Phase Inverter operated by DSP

Saidi Hemza

*Electrical Engineering Department, Mohamed Boudiaf University of Science and Technology, Oran, Algeria;
E-mail: h.saidi@univ-chlef.dz*

Midoun Abdelhamid

*Electrical Engineering Department, Mohamed Boudiaf University of Science and Technology, Oran, Algeria;
E-mail: ah_midoun@hotmail.com*

Noureddine Mansour

*College of Engineering University of Bahrain P.O. Box 32038, Kingdom of Bahrain
E-mail: nmansour@uob.edu.bh*

Abstract

Solar electric vehicles (SEV) are considered the future vehicles to solve the issues of air pollution, global warming, and the rapid decreases of the petroleum resources facing the current transportation technology. However, SEV are still having important technical obstacles to overcome. They include batteries energy storage capacity, charging times, efficiency of the solar panels and electrical propulsion systems. Solving any of those problems and electric vehicles will compete-complement the internal combustion engines vehicles.

In the present work, we propose an electrical propulsion system in order to obtain the desired speed and torque with less power loss. Because of their lightweight nature, small volume, low cost, less maintenance and high efficiency, a three phase squirrel cage induction motor (IM) is selected for the electrical propulsion system. The IM is fed from three phase inverter which is operated by Space Vector Pulse Width Modulation (SVPWM) technique. The proposed system uses Texas Instruments TM320F2812 Digital Signal Processor (DSP) to generate SVPWM signal needed to trigger the gates of IGBT-based inverter. The experimental results show the ability of the proposed system to generate a three-phase sine wave signal with desired frequency. The system is also experimented on SEV prototype which we manufactured and the results show that the EV prototype can be propelled to speed up to 60 km/h under different road conditions.

Keywords: Solar Car, DSP, electric vehicle, hybrid power system.

Introduction

Algeria is among the firsts countries producing oil and gas. And that doesn't prevent the government to implement a policy for the development of Renewable Energies (RE) and adopt gradually mix energy. The objective is to attain 40% of its electricity production from renewable energy source, by 2030, according to its international commitments, to protect the planet.

In this context, efforts to improve air quality in heavily populated urban communities-by reducing vehicular emissions – have rekindled interest in the development of electric vehicle technology. However, the key issues which are challenging the design of electric vehicles are the electric

propulsion system, energy sources and battery management system [1]. Solving any of those issues and electric vehicles will compete-complement the conventional internal combustion engines vehicles.

This paper will focus only on the electric propulsion system design and will investigate its key components including the electric motor, the inverter and the processor based control system.

DC motor drives have been widely applied to EVs because of their technology maturity and control simplicity. However, at present squirrel cage AC induction motors are considered the mature technology among the commentator less motor drives. Compared to DC motor drives, the AC induction motors have lightweight, small volume, low cost, less maintenance and high efficiency. These advantages are particularly important for EV applications.

As EVs propulsion, an AC induction motor drive is fed with a DC source (battery), which has approximately constant terminal voltage. Thus a variable frequency and variable voltage DC/AC inverter is needed to feed the induction motor. The DC/AC inverter is constituted by power electronic switches and power diodes. The current generation of inverter is based on high speed power transistors, like IGBT and MOSFET and high speed SCR, like GTO. As results of this improvement of fast switching semiconductors, variable-frequency drives made speed control of an AC induction motor easier.

Since the output of the inverter is a high frequency square wave, a high speed processor is needed to produce the proper switching sequence. Various switching techniques [2] are used to generate PWM signal which is used to determine the amplitude and the frequency of the output voltage. Among the various PWM techniques, Space Vector Pulse Width Modulation (SVPWM) has advantages that made it the most switching techniques used in power converters [3].

The interesting feature of this type of modulation is that it can be easily implemented on digitally and hence offer the advantage to perform entire digital processing. The performance of SVPWM depends on the type of processor used for its implementation. Among the various processors available in the market, the most popular are the Texas Instrument DSP which hold about 70% of the market. TMS320F2xxx DSP series are high speed processors which have been developed by Texas Instruments especially for

industrial control applications, in particular for implementation of SVPWM algorithm to drive the switches of the inverter and AC induction motor speed control.

The objective of this study is to develop an electric propulsion system based on three phase squirrel cage induction motor, IGBT-based three phase inverter and advanced processor, such as DSP, implementing SVPWM algorithm for open loop speed control of solar electric vehicle. The paper is organized as follows: first we discuss the SVPWM technique, second we discuss the mechanical part of the vehicle, and third we describe the electrical propulsion system and finally practical results obtained are presented along with conclusions.

2 Space Vector Pulse Width Modulation Techniques

A number of Pulse width modulation (PWM) schemes are used to control the magnitude and frequency of AC output voltage of the inverter. The most widely used PWM schemes for three-phase voltage source inverters are sine wave sinusoidal SPWM and space vector PWM (SVPWM). Since SVPWM is easily implement digitally, more efficient utilization of DC bus voltage, and generate sine wave with lower total harmonic distortion, it is most frequently preferable technique used in modern AC machines drives fed by inverters.

Although SVPWM is more complicated than sinusoidal PWM, it may be implemented easily with modern DSP based control systems. The space vector PWM technique implemented into the existing TI Digital Motor Control (DMC) library reduces the number of transistor commutations. It therefore improves EMI behavior.

3 Space vector concepts:

The space vector concept, which is derived from the rotating field of induction motor, is used for modulating the inverter output voltage. In this modulation technique the three phase quantities can be transformed to their equivalent two-phase quantity either in synchronously rotating frame (or) stationary frame. From these two-phase components, the reference vector magnitude can be found and used for modulating the inverter output. The process of obtaining the rotating space vector is explained in the following section. Considering the stationary reference frame let the three-phase sinusoidal voltage output component be,

$$\begin{pmatrix} v_{AN} \\ v_{BN} \\ v_{CN} \end{pmatrix} \quad (1)$$

When this three-phase voltage is applied to the AC machine it produces a rotating flux in the air gap of the AC machine. This rotating resultant flux can be represented as single rotating voltage vector. The magnitude and angle of the rotating vector can be found by means of Clark's Transformation as explained below in the stationary reference frame. To implement the space vector PWM, the voltage equations in the abc reference frame can be transformed into the stationary α - β reference frame that consists of the horizontal (α) and vertical (β) axes. The components of

$[v_A, v_B, v_C]^T$ in the α - β are $[v_\alpha, v_\beta, v_0]^T$. They are related as follows:

$$\begin{bmatrix} v_{s\alpha} \\ v_{s\beta} \end{bmatrix} = \sqrt{\frac{2}{3}} \cdot \begin{bmatrix} 1 & -\frac{1}{2} & -\frac{1}{2} \\ 0 & \frac{\sqrt{3}}{2} & -\frac{\sqrt{3}}{2} \end{bmatrix} \cdot \begin{bmatrix} v_{AN} \\ v_{BN} \\ v_{CN} \end{bmatrix} \quad (2)$$

Where, the component v_0 is null.

As described in figure, this transformation is equivalent to an orthogonal projection of $[a \ b \ c]^T$ onto the two-dimensional perpendicular to the vector $[1 \ 1 \ 1]^T$ (the equivalent d-q plane) in a three-dimensional coordinate system. As a result, six non-zero vectors (V1-V6) and two zero vectors (V0 and V7) are possible. Six non-zero vectors (V1-V6) shape the axes of a hexagonal as depicted in Figure-3, and supplies power to the load. The angle between any adjacent two non-zero vectors is 60 degrees. The eight vectors are called the basic space vectors and are denoted by (V0, V1, V2, V3, V4, V5, V6, and V7). The same transformation can be applied to the desired output voltage to get the desired reference voltage vector, V_s in the d-q plane.

The objective of SVPWM technique is to approximate the reference voltage vector V_s using the eight switching patterns. One simple method of approximation is to generate the average output of the inverter in a small period T to be the same as that of V_s in the same period.

For 180° mode of operation, there exist six switching states and additionally two more states, which make all three switches of either upper arms or lower arms ON. To code these eight states in binary (one-zero representation), it is required to have three bits ($2^3 = 8$). And also, as always upper and lower switches are commutated in complementary fashion, it is enough to represent the status of either upper or lower arm switches.

Let "1" denote the switch is ON and "0" denote the switch in OFF.

The algorithm of SVPWM could be summarized in the following two main steps [4]:

Space vector PWM can be implemented by the following steps:

Step-1: Determine $V_{s\alpha}$, $V_{s\beta}$, V_s and δ through the following equations which use abc to $\alpha\beta$ Clark transformation.

From figure, $V_{s\alpha}$, $V_{s\beta}$, V_s and δ can be determined as follows:

$$v_{s\alpha} = r \cdot \sqrt{\frac{3}{2}} \cdot \frac{E}{2} \cdot \cos \delta \quad (3)$$

$$v_{s\beta} = r \cdot \sqrt{\frac{3}{2}} \cdot \frac{E}{2} \cdot \sin \delta \quad (4)$$

$$|\vec{V}_s| = \sqrt{v_{s\alpha}^2 + v_{s\beta}^2} \quad (5)$$

$$\delta = \tan^{-1} \frac{v_{s\beta}}{v_{s\alpha}} = 2\pi f_s t \quad (6)$$

Where, f_s is the fundamental frequency.

At each instant, the vector V_s be expressed as linear combination of two vectors $V_{s(k)}$ and $V_{s(k+1)}$ that are adjacent to it. For example at Sector-1 ($0 \leq \delta \leq \pi/3$), we have

$$\vec{V}_s = \frac{\sqrt{3}}{2} \cdot r \cdot \sin\left(\frac{\pi}{3} - \delta\right) \cdot \vec{V}_1 + \frac{\sqrt{3}}{2} \cdot r \cdot \sin \delta \cdot \vec{V}_2 \quad (7)$$

Step-2: Determine the time duration T_1 , T_2 and T_0
We can calculate the switching time duration in each sector of the hexagon using where the realized calculation below is for Sector-1. In figure A_1 and A_2 are cyclic ratio of the vector V_1 and V_2 respectively and expressed as:

$$A_1 = \frac{T_1}{T} \vec{V}_1$$

$$A_2 = \frac{T_2}{T} \vec{V}_2 \quad (8)$$

Using the above, we can derive T_1 and T_2 as follows:

$$T_1 = \frac{\sqrt{6} \cdot V_{s\alpha} - \sqrt{2} \cdot V_{s\beta}}{2E} T \quad (9)$$

$$T_2 = \frac{\sqrt{2} \cdot V_{s\beta}}{E} \cdot T \quad (10)$$

$$T_0 = T - T_1 - T_2 \quad (11)$$

By making the same calculation for each sector, the **figure** below is obtained [1] which can be used to determine the switching time of each IGBT (K1 to K6).

4 Vehicle Body Developments and Requirement

Figure1 is used to derive the desired driving power to ensure vehicle operation [5]. The mechanical structure of the solar vehicle prototype manufactured is shown in figure 2. The weight, volume and aerodynamic drag and rolling resistance effects have been considered in the design of the body of the vehicle. The desired performance required for the prototypes manufactured is to attain maximum speed of 60 km/h and vehicle total charge of 500 gh.

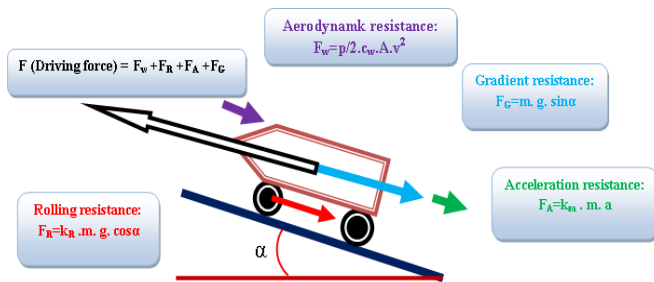


Fig. 1. Representation of all forces acting

The road slope torque T is defined by:

$$T_w = \frac{p}{2 \cdot c_w} \cdot A \cdot v^2 \quad (12)$$

$$T_R = k_R \cdot m \cdot g \cdot \cos \alpha \quad (13)$$

$$T_A = k_m \cdot m \cdot a \quad (14)$$

$$T_G = m \cdot g \cdot \sin \alpha \quad (15)$$

$$T = T_w + T_R + T_A + T_G$$

Where; T_w is aerodynamic torque, T_R : rolling torque, T_A acceleration torque and T_G gradient torque.

Torque evaluation of the power flow occurring into a vehicle is in strong relation with its mass and a total couple will be expressed as:

$$C_t = T_A + T_{permanent} \quad (16)$$

Where; m is a vehicle mass, C_t total torque, T_A acceleration torque, $T_{permanent}$ permanent torque, α road angle.

For this study, we used for the EVs propulsion a cage three phase induction motor of 4.7 kW 220/380 V 11/19 A with maximum speed of 1500 rpm. The solar panel station to refuel the vehicle batteries are shown in figure3.



Fig. 2. The second car manufacturer



Fig. 3. Solar charging unit manufacturer

5 Description of the Electrical Propulsion System

Figure 4 shows the block diagram of the open loop control system used to adjust the speed of the vehicle. The hardware includes squirrel cage induction motor, bridge inverter, isolation card, Digital Signal Processor (DSP), speed sensor, potentiometer for desired speed adjustment, and switches for user interface.

The desired speed is entered by the user via the potentiometer and converted to digital signal using digital to analog converter in order to enter it to the DSP.

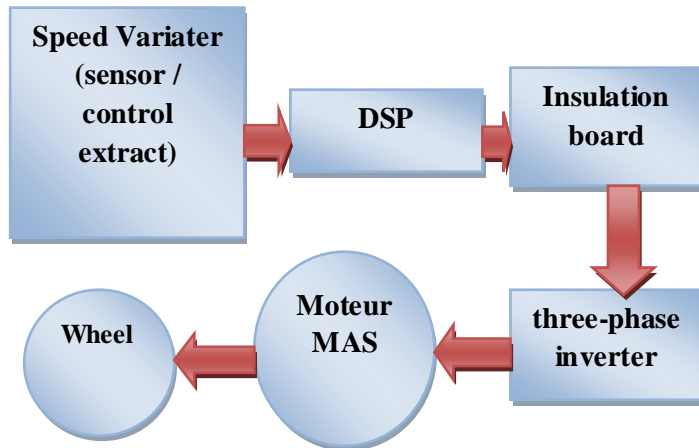


Fig.4. the block diagram of the open loop control system.

6 Hardware Specifications

6-1 Digital Signal Processor (DSP):

it is a 32-bit 150MIPS TMS320F2812 DSP developed by Texas Instruments Inc. It is used to generate PWM signals. CCS (Code Composer Studio v2) provided by Texas Instruments is used [6].

6-2 Isolation Card it is used:

to ensure the necessary galvanic isolation between DSP and power inverter. It is a rapid optocoupler of HCLP 2601 type. In addition to the galvanic isolation, it provides also signal inversion and amplification.

6-3 IGBT-based Three Phase Inverter:

it is an International Rectifier's IRAMY20UP60B type 20A, 600V Integrated Power Hybrid IC (HIC) with Internal Shunt Resistor. This offers an extremely compact, high performance AC motor-driver in a single isolated package to simplify design. This advanced HIC is a combination of IR's low VCE (on) Non Punch-Through IGBT technology and the industry benchmark 3-Phase high voltage, high speed driver in a fully isolated thermally enhanced package. A built-in temperature monitor and over-current and over-temperature protections, along with the short circuit rated IGBTs and integrated under-voltage lockout function, deliver high level of protection and failsafe operation. Using a new developed single in line package (SiP3) with heat spreader for the power die along with full transfer mold structure minimizes PCB space and resolves isolation problems to heat sink.

6-4 Three Phase Squirrel Cage induction Motor

4.7 KW, 3 phase, 220/380V, 11/19A, 1500 rpm, 2 pair of poles DC batteries(12v/48Ah) and Solar panel (220w/48v).

6-5 Open Loop Control Algorithm:

The user adjusts the desired speed using a potentiometer and this latter convert it to its analogous voltage. The output of the potentiometer is inputted to the DSP as digital signal using

ADC converter. The open loop control program consists of several stages as shown in the flow chart depicted in figure 6. Based on figure, the open loop system can be summarized as follows:

- Initialization DMC modules and declare variables
- Determine V_s voltages with constant V/F profile
- Determine the time durations T_a , T_b and T_c using SVPWM module
- Generate the signal PWM based on the time durations T_a , T_b and T_c .

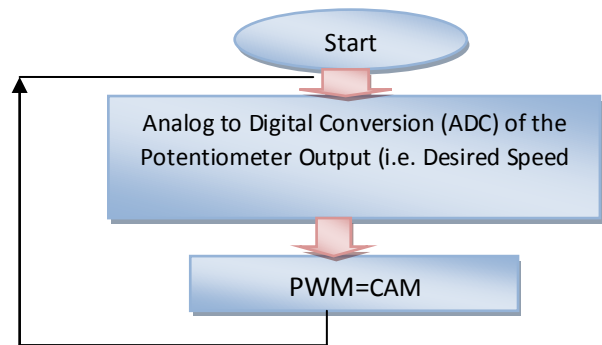


Fig. 5. Program of PWM

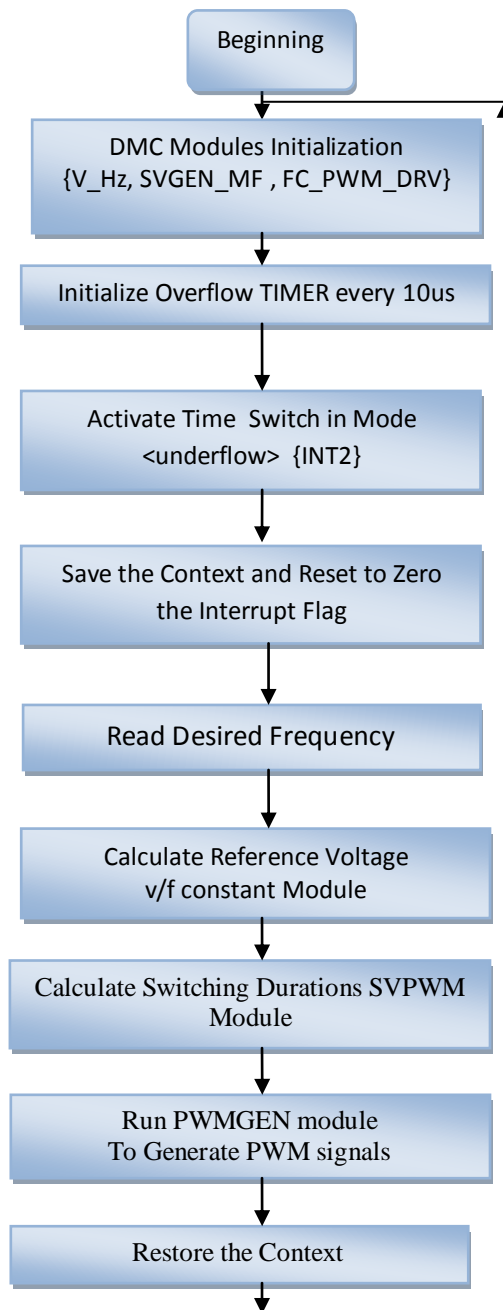


Fig.6. Program Flow.

7 Practical Results

Figures 7 show the PWM signals generated by the SVPWM module after the execution of the program developed. Figure 8 illustrates the two PWM pulses which are complementary and used to trigger the gates of one leg of the IGBT bridge of the inverter. As shown in figure 9, in order to avoid the short circuit of inverter power supply, we introduced a time delay of 0.5 μ s between the two complementary pulses.

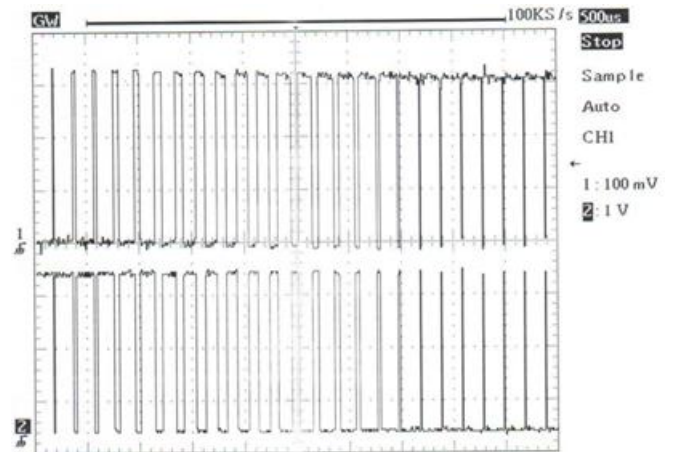


Fig. 7. PWM signal and its complement.

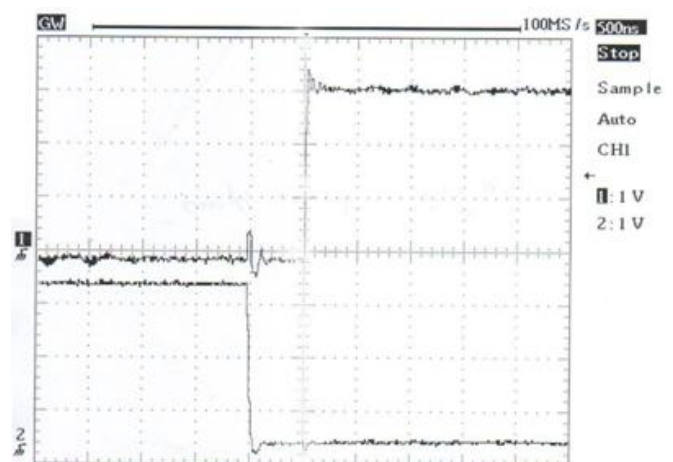


Fig. 8. Dead time between two complementary pulses.

PWM signals before and after the optocoupler. The voltage magnitude of PWM generated by the DSP is 3.3 volts which are inputted to the optocouplers are inverted and amplified to 5 volts. To check the switching behavior and the reliability of the IR IRAMY20UP60B module, we investigated the operation of one of its cell during commutation. Figure 11 illustrates the waves of current and tension for an IGBT cell under RL inductive load with $R=8.4 \Omega$ and $L=4.75 \text{ mH}$ during commutation. The switching frequency of the IGBTs transistors and DC power supply voltage are 10 kHz and 160 V respectively. As shown in figure, the current increases in continuous form from 0 to 5 A during switching off (Switch Open) and then decreases back to 0 A during. Switching on (Switch Close). The voltage across the switch is equal to the DC power supply. Figure 11 shows small voltage spikes and current ringing during switching which are probably due to the IGBTs internal parameters. The inverter is tested to supply induction motor with rating 4.7KW with and without load. This latter is selected to move the vehicle. The switching frequency of the IGBTs transistors and DC power supply voltage are 10 kHz and 200 V respectively. Results illustrated in figure 12 and 13 show the current and line to neutral voltage at the inverter output when

supplying the motor. As can be noticed, the current wave is almost sinusoidal and the harmonics are due probably to internal parameter of the inverter. Figure also shows the ability of the inverter change speed of the motor (i.e. Vehicle) by generate sinusoidal voltage for different desired frequencies (i.e. 25 Hz and 50Hz).

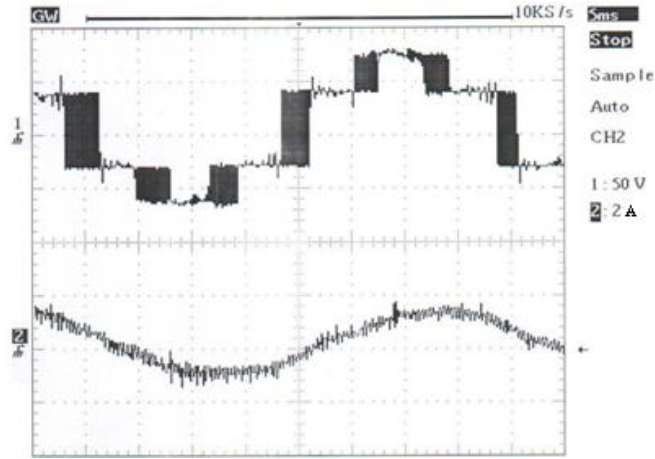


Fig. 9. waveform of the phase voltage and phase current for $f = 25\text{Hz}$ with a load torque.

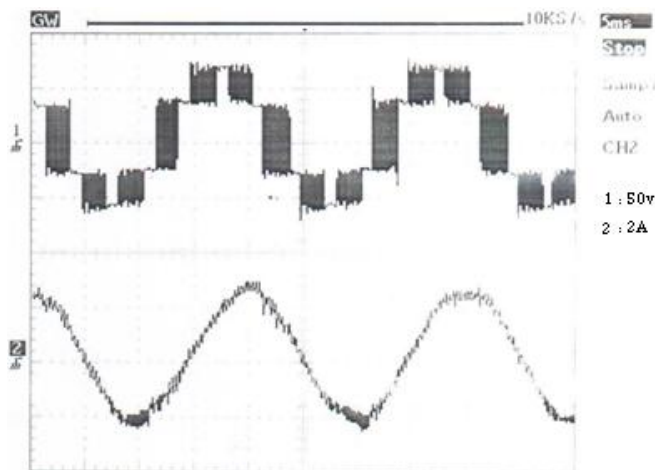


Fig.10. waveform of the phase voltage and phase current for $f = 50\text{Hz}$ with a load torque.

Finally, we investigate the practical performance of the electric propulsion system designed under road load. The vehicle has been operated on flat road and we started changing its speed at different stages. The results obtained are very satisfactory as shown in **figure 11**. The maximum speed reached is about 60 Km/h.

The capability of the electric propulsion system under overload was also investigated by operating the vehicle on graded road condition where the road grade angle is about 45 degree. The results are shown in **figure 12**. The speed reached in this case is about 45 km/h

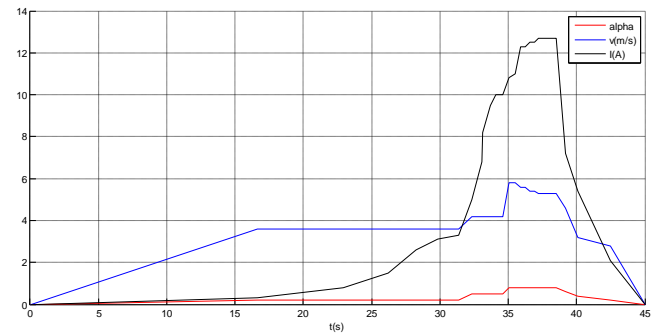


Figure 11: Using the vehicle in a horizontal Course.

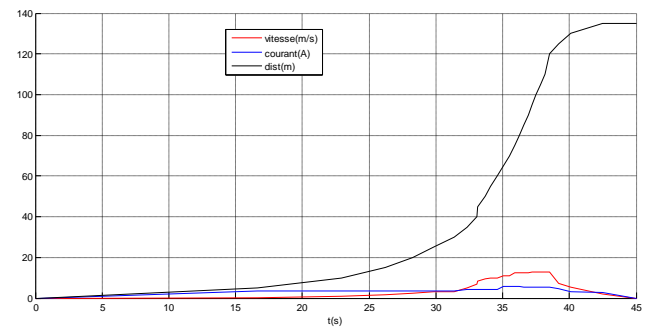


Fig. 12. Using the car in italic Course.

Conclusions

The paper presents design of an electric vehicle which is propelled by three phase cage induction motor and powered by solar energy. After several experiment performed, we demonstrated that the DSP-based control system developed is able to operate the vehicle at different speeds and under flat and uphill road condition. However, some difficulties have been encountered during the startup. This is probably due to the inappropriate choice of the induction motor power. Because using DC motor on the same vehicle, we did not encounter any problem of startup. Therefore, more attention is required in the selection of the most appropriate induction motor. In fact, the choice of electric propulsion systems for EVs mainly depends on three factors: driver expectation, vehicle constraint, and energy source. Due to its low cost, robustness, highly reliable and free from maintenance, automobile industry will certainly select cage induction motor as the most appropriate candidate to achieve these requirements. Hence, we believe that the work carried out will contribute in development of future electric vehicles based on cage induction motor.

References

- [1] livre de saidi hemza titre « Etude et réalisation de véhicule solaire » en Allemagne (Edition universitaires européens) ISBN : 978-613-1-55909-9.
- [2] LLOR.M.A.-Commande directe de couple à fréquence de modulation constante des machines synchrones à

- aimants permanents. Thèse de doctorat, université INSA, Lyon, France. 2003.
- [3] GRELLET.G et CLERC.G.-Actionneurs électriques : Principes, modèles et commandes. Eyrolles, Paris, France. 2000.
- [4] HAMIDI.A et HIRECHE.A.-Étude comparative entre la commande à MLI vectorielle et la commande à MLI sinus-triangle d'un onduleur à deux niveaux de tension. Mémoire d'ingénieur, centre universitaire D' M.Tahar, Saïda, Algérie. 2002.
- [5] Règlement Technique Energie Alternative / Alternative Energy Technical Regulations. FIA Sport / Technical Department. 11.12.2006.
- [6] DEWIT.C.C.-Modélisation, contrôle vectoriel et DTC : Commande des machines asynchrones. Hermes Science Europe Ltd. 2000.
- [7] B. Mehdi, S. Mikael, P. Thomas« véhicule semi-automatique et algorithme d'évitement d'obstacle » Projet 15, Laboratoire COSI-Majeur Systèmes Embarqués – 2003.